PLOS ONE

RESEARCH ARTICLE

Ganglion cells and displaced amacrine cells density in the retina of the collared peccary (*Pecari tajacu*)

Kelly Helorany Alves Costa[1,2], Bruno Duarte Gomes[1], Luiz Carlos de Lima Silveira[1,2,3†], Givago da Silva Souza[2], Isabelle Christine Vieira da Silva Martins[1], Eliza Maria da Costa Brito Lacerda[3], Fernando Allan de Farias Rocha[1]*

1 Instituto de Ciências Biológicas, Universidade Federal do Pará, Belém, Pará, Brasil, **2** Núcleo de Medicina Tropical, Universidade Federal do Pará, Belém, Pará, Brasil, **3** Universidade CEUMA, São Luís, Maranhão, Brasil

† Deceased.
* rochaf@ufpa.br

Citation: Costa KHA, Gomes BD, Silveira LCdL, Souza GdS, Martins ICVdS, Lacerda EMdCB, et al. (2020) Ganglion cells and displaced amacrine cells density in the retina of the collared peccary (*Pecari tajacu*). PLoS ONE 15(10): e0239719. https://doi.org/10.1371/journal.pone.0239719

Editor: Tudor C. Badea, National Eye Centre, UNITED STATES

Received: June 9, 2020

Accepted: September 11, 2020

Published: October 1, 2020

Data Availability Statement: All relevant data are within the paper and its Supporting Information files.

Funding: This work was supported by research grants from Brazilian funding Conselho Nacional de Desenvolvimento Científico e Tecnológico (CNPq): CNPq/Universal #459499/2014-9 (FAFR and BDG); CNPq/Universal #436717/2018-2 (BDG and FAFR); CNPq #431748/2016-0 GSS is CNPq Fellow. http://cnpq.br/. The funders had no role in study design,

Abstract

In the present study, we investigated the topographical distribution of ganglion cells and displaced amacrine cells in the retina of the collared peccary (*Pecari tajacu*), a diurnal neotropical mammal of the suborder Suina (Order Artiodactyla) widely distributed across central and mainly South America. Retinas were prepared and processed following the Nissl staining method. The number and distribution of retinal ganglion cells and displaced amacrine cells were determined in six flat-mounted retinas from three animals. The average density of ganglion cells was 351.822 ± 31.434 GC/mm^2. The peccary shows a well-developed visual streak. The average peak density was 6,767 GC/mm^2 and located within the visual range and displaced temporally as an area temporalis. Displaced amacrine cells have an average density of 300 DAC/mm^2, but the density was not homogeneous along the retina, closer to the center of the retina the number of cells decreases and when approaching the periphery the density increases, in addition, amacrine cells do not form retinal specialization like ganglion cells. Outside the area temporalis, amacrine cells reach up to 80% in the ganglion cell layer. However, in the region of the area temporalis, the proportion of amacrine cells drops to 32%. Thus, three retinal specializations were found in peccary's retina by ganglion cells: visual streak, *area temporalis* and dorsotemporal extension. The topography of the ganglion cells layer in the retina of the peccary resembles other species of Order Artiodactyla already described and is directly related to its evolutionary history and ecology of the species.

Introduction

The Amazon rainforest is the most biodiverse biome of the planet. It is the home of many animal species, including mammals, thus being a significant source of data for comparative anatomy and physiology of tropical wildlife. Throughout the years, several studies have focused on the visual system morphophysiological organization in rodents and primates [1–22].

data collection and analysis, decision to publish, or preparation of the manuscript.

Competing interests: The authors have declared that no competing interests exist.

The Order Artiodactyla has been the target of many studies that aimed to characterize the morphology and physiology of retinal cells. Methods that used morphological and electrophysiological analysis have shown a dichromatic vision supported by short and medium-wavelength sensitive cone cells [23–29]. More specifically, in the ganglion cells layer, the topography distribution was studied in species such as the domestic pig–*Sus scrofa* [30, 31], the giraffe—*Giraffa camelopardalis* [32], Hippopotamus—*Hippopotamus amphibius* [33] goat —*Murciano-granadina breed* [34], and the sheep—*Ovis aries* [35]. These species presented similar topographical ganglion cells distribution: the presence of a high cellular density region elongated horizontally and situated above the optic disc, known as visual streak; a density peak along the visual streak that is temporally dislocated and known as *area temporalis* [36]. This spatial variation of the cell density was also observed for the photoreceptors cone type with short and medium wavelengths in the retina of pigs [29].

The collared peccary (*Pecari tajacu*) is a neotropical mammal of the suborder Suina (Order Artiodactyla), morphologically similar to the suidae of the Old World [37] The collared peccary is widely distributed across central and mainly South America. They have a diurnal/crepuscular activity, feeding in the early to mid-morning and late afternoon to the early hours of the night [38]. For peccary, Ahnelt et al., pointed out that peccaries and suits have similar photoreceptor morphology with rods and cones area easily distinguishable [28]. Furthermore, cones had a high concentration in temporal retina of which the S cones, were arranged in a random mosaic and comprised 10% of the total cone cell population as it is observed for that type of cone in other mammals [28]. Recently, Ezra-Alia et al., have reported more detailed aspects of the peccary retina. They showed that the amount of M/L cones is greater than S cones, and that the amplitude of the combined response of cones and rods is smaller compared to domestic pigs, but very similar to minipigs [39].

The characterization of the ganglion cell distribution and density is still missing for the collared peccary. Thus, in the present study, we aimed to fill this gap using whole-mounted retinas and Nissl staining to investigate the ganglion cell topography of the collared peccary.

Materials and methods

Ethical aspects

Experiments were performed with three adults collared peccary (*P. tacaju*), all males. With the weight between 15–22 kg and age about 2.5 years (±0.6). The animals were obtained from Empresa Brasileira de Pesquisa Agropecuária—Embrapa/Pará. The maintenance and handling procedures were reviewed and approved by the research ethics committee of the Universidade Federal do Pará (CEPAE, N˚ 034–2015).

Animals

The peccaries were euthanized with a 50 mg/kg lethal intraperitoneal injection of sodium thiopental (Thionembutal, Abbott, São Paulo, Brazil) and later the eyes were removed for the present research. The eyes were enucleated immediately after death, cornea and lens were removed. Eyecups were fixed by immersion in 10% formaldehyde in 0.1 M phosphate buffer, pH 7.4. After fixation, whole mounts of the retina were prepared and processed following the Nissl staining method [15, 32, 40]. For retinal orientation first the optic nerve was identified by its conspicuous oval appearance and temporal displacement. Next, five cuts were performed as follow, one cut at each nasal and temporal ends just below the optic nerve, one cut at the ventral end and two cuts in the ends of the diagonal direction.

For the technique described above only six retinas from three animals (all male) were used, firmly adhered to vitreal side up in gelatinized slice, was incubated in formaldehyde vapors for

two hours at 60 ºC. Next, the retina was washed in distilled water and stained with 0.5% cresyl violet for 10 min and dehydrated in a series of graded ethanol concentrations, cleared in xylene and coverslipped with Permount.

Imaging and analysis

The ganglion and amacrine cells were viewed and digitally documented using a microscope Axion Scope A1 (Carl Zeiss) with camera Axiocam HRc. The cell counting was made directly in the microscope using square fields and an objective A-plan 100x/1.25 Oil (Carl Zeiss). The cells were counting at 1 mm intervals along two meridians: (1) horizontal, in the naso-temporal axis along the visual streak; (2) vertical, dorsal-ventral axis, which crosses the horizontal meridian and the optic disc perpendicularly. Counts were also made along the vertical meridian from temporal to nasal border. For some special-target areas, as the *visual streak* or *area temporalis*, the interval between the counting fields was 0.5 mm and 0.25 mm, respectively.

The ganglion and amacrine cell counts were converted to density in cells/mm^2, and the estimation of the isodensity lines was described in earlier studies of our group [15, 21]. Briefly, the isodensity contours were plotted linking the points over an isodensity contour and the points located between densities higher and lower than that corresponding to the isodensity contours. The total number of ganglion cells (GC) and displaced amacrine cells were then obtained by a simple measure of the area between two isodensity contours multiplying the area times the mean density value of the two isodensity contours. The total number was then the sum of all the resulting isodensity figures. To color the topographic maps the isodensity contours were drawn and converted into color-coded isodensity lines using SigmaPlot® for Windows™ Version 12.5 software (Systat Software, Inc., Richmond, CA).

Statistical analysis

For descriptive statistics and plotting of Figs 5, 6, 7 and 9, we used the SigmaStat® for Windows™ Version 3.11 program (Systat Software, Inc., Richmond, CA).

Results

Gross anatomy, retinal area and identification of ganglion cells and displaced amacrine cells

The peccary's retina had a typical vascular pattern called holangiotic as early described [39], the optic disc (OD) has an oval appearance. It is located just below the center of the retina and temporally displaced (Fig 1). The retinal area comprised 837.8 ± 56.5 mm^2 (N = 6) before the histological procedure and 828.8 ± 52.3 mm^2 after the histological procedure. The shrinkage due to histological procedures was estimated and ranged from 0.40% to 1.87%, a compilation of retinal area measurements performed before and after histology is showed on Table 1. The shrunken area was restricted to the periphery. Thus, ganglion cell counting was completed with no corrections for shrinkage.

We used morphological criteria to differentiate ganglion cells from neuroglial cells and displaced amacrine cells according to Hughes [41] The same criteria was used in other studies for artiodactyls species [32, 42, 43] and other species [17, 40, 44]. Briefly, ganglion cells have a large soma with an oval pale nucleus and a prominent nucleolus with abundant Nissl substance visible in the cytoplasm. On the other hand, displaced amacrine cells have small soma and cytoplasm containing less Nissl (Fig 2).

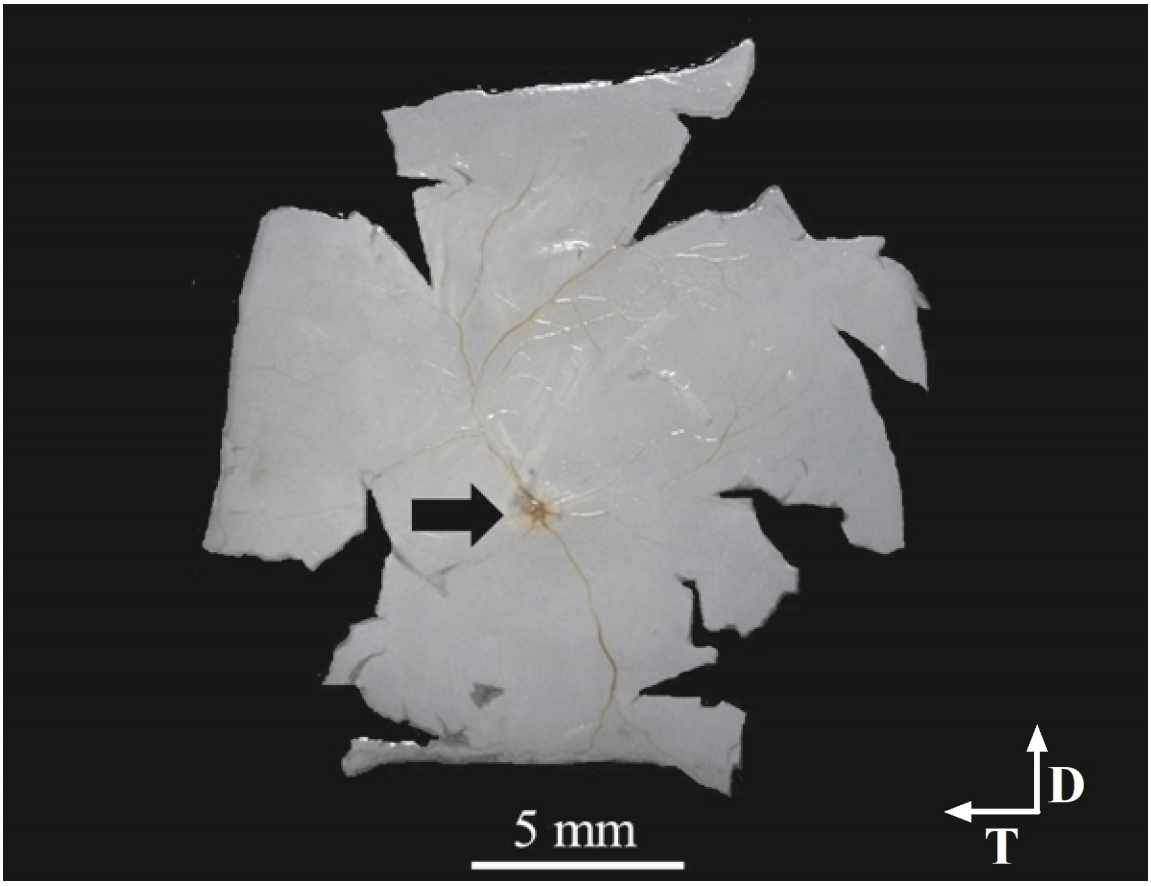

Fig 1. Wholemount retina of peccary. The retina was flattened on gelatin-coated slides right after the histological dissection. Blood vessels can be seen converging to the optic disc to where the arrow is pointed.

https://doi.org/10.1371/journal.pone.0239719.g001

Total number and topography of ganglion cells

The total of the ganglion and displaced amacrine cells was estimated by the integration of isodensity contours from the isodensity maps (Fig 3). The total number of ganglion cells for all retinas was 1,029,498 (±121,060) (Table 1). Table 2 shows the descriptive statistic for the density of ganglion cells; the mean density for all retinas analyzed was 2254 GC/mm^2 (± 346.7). The animal 03 showed the lower values, around 1,990 GC/mm^2 for both retinas. The density peak also varied strongly, the highest value was 9,900 GC/mm^2, and the lower value was 5,100 GC/mm^2, with peak mean at 6,767 GC/mm^2 (±1,914).

When we analyzed the ganglion cell isodensity maps (Fig 3), it can be seen that the lower cellular density occurred at the retinal periphery and was around 500 GC/mm^2. The density increases concentrically towards the visual streak with density contours varying from around 2000 to 4000 GC/mm^2. Besides, in visual streak, there was a temporarily dislocated circular region with densities between 4000 and 5000 GC/mm^2, inside this area it´s located the peak density (*), this area is called *area temporalis* [36]. Fig 4 shows the "average" isodensity map for all retinas used in this study. For the "average" map, the isodensity contours were drawn from mean density values of six retinas and plotted on the map of Animal 03 (left retina). Here we analyzed the number of ganglion cells by region. Each region was defined for lines isodensity contours. Thus, region ***A*** corresponded to the area between the wholemount border and the 500 GC/mm^2 contour. The ***B*** region is the area between 500 and 1000 GC /mm^2; ***C*** region

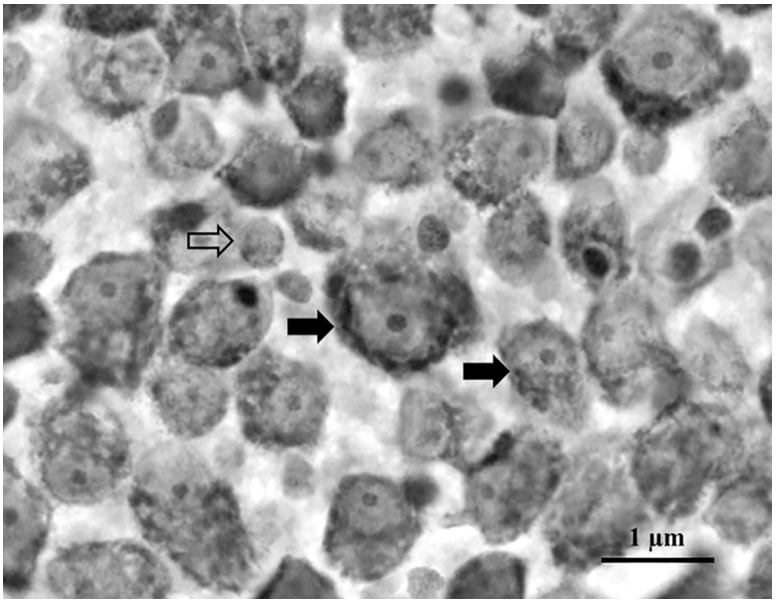

Fig 2. Nissl-stained of the whole-mounted retina. Ganglion cells are indicated by filled arrows and displaced amacrine cells by the empty arrow. Ganglion cells have a large soma with pale nucleus and nucleolus with abundant Nissl substance. Displaced amacrine cells have small soma and cytoplasm containing less Nissl substance. Scale bar = 1µm.

https://doi.org/10.1371/journal.pone.0239719.g002

was the area between 1000 and 2000 GC/mm^2; ***D*** region was the area between 2000 and 3000 GC/mm^2; ***E*** region was the area between 3000 and 4000 GC/mm^2; ***F*** region was the area between 4000 GC/mm^2 and density peak area represent by (*). In Fig 5 we presented a column graphic compared to the number of ganglion cells by region identify in the "average" isodensity map showed in Fig 4. Here we do not consider the density peak for this comparison. We observed that the region with most ganglion cells was ***C,*** followed for the ***B*** and ***D*** region.

The Figs 6 and 7 show the ganglion cells density profile in the dorsal-ventral and temporal-nasal axes, respectively. For the dorsal-ventral axis (Fig 6) the peak density was temporarily located at a mean distance of 3.13 mm (± 0.38) from the dorsal region to the optic nerve. The peak density varied among retinas with values ranging from 5100 to 9900 GC/mm^2 (Table 2). From the optic nerve, there is an abrupt decrease in cell density to values close to 1000 GC/mm^2 in the dorsal and ventral. Similarly, in the dorsal and ventral periphery, especially between the retinal border and first-line contour, the density falls to about 500 GC/mm^2.

For the temporal-nasal axis, along the visual streak (Fig 7), the density was around 4000 GC/mm^2 from nasal to central direction. The peak density was temporarily located at approximately 6.77 mm (± 0.60) from the optic nerve.

Displaced amacrine cells

The topographical distribution of displaced amacrine cells (DAC) differs significantly from the ganglion cells distribution in two critical aspects: First, there was no spatial arrangement such as a visual streak; second, there was a significant decrement of displaced amacrine cells in the *area temporalis* (Fig 8). The distribution of displaced amacrine cells is homogeneous in the majority of the retina (Fig 8B) with a density of around 3000 DAC/mm^2, and in the *area temporalis* region (white stippled circle), there was a considerable decrease in the density of displaced amacrine cells.

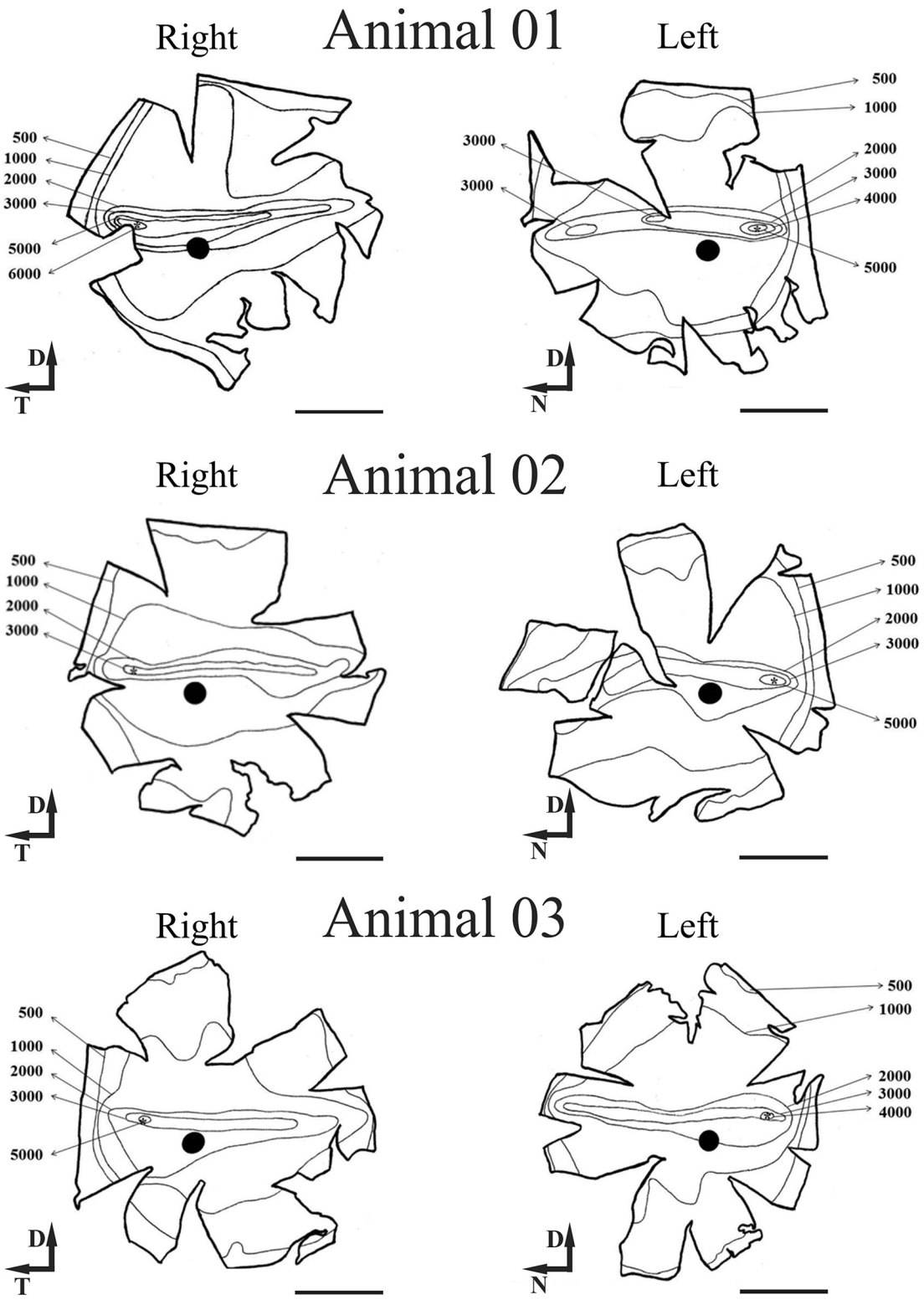

Fig 3. Ganglion cell isodensity maps for peccary's retina. The contours correspond to the isodensity lines. The visual streak is visible by the horizontal elongation of the contours in the centro-dorsal retina. (*) Peak density local, (•) optic disc. Scale bar = 5 mm.

https://doi.org/10.1371/journal.pone.0239719.g003

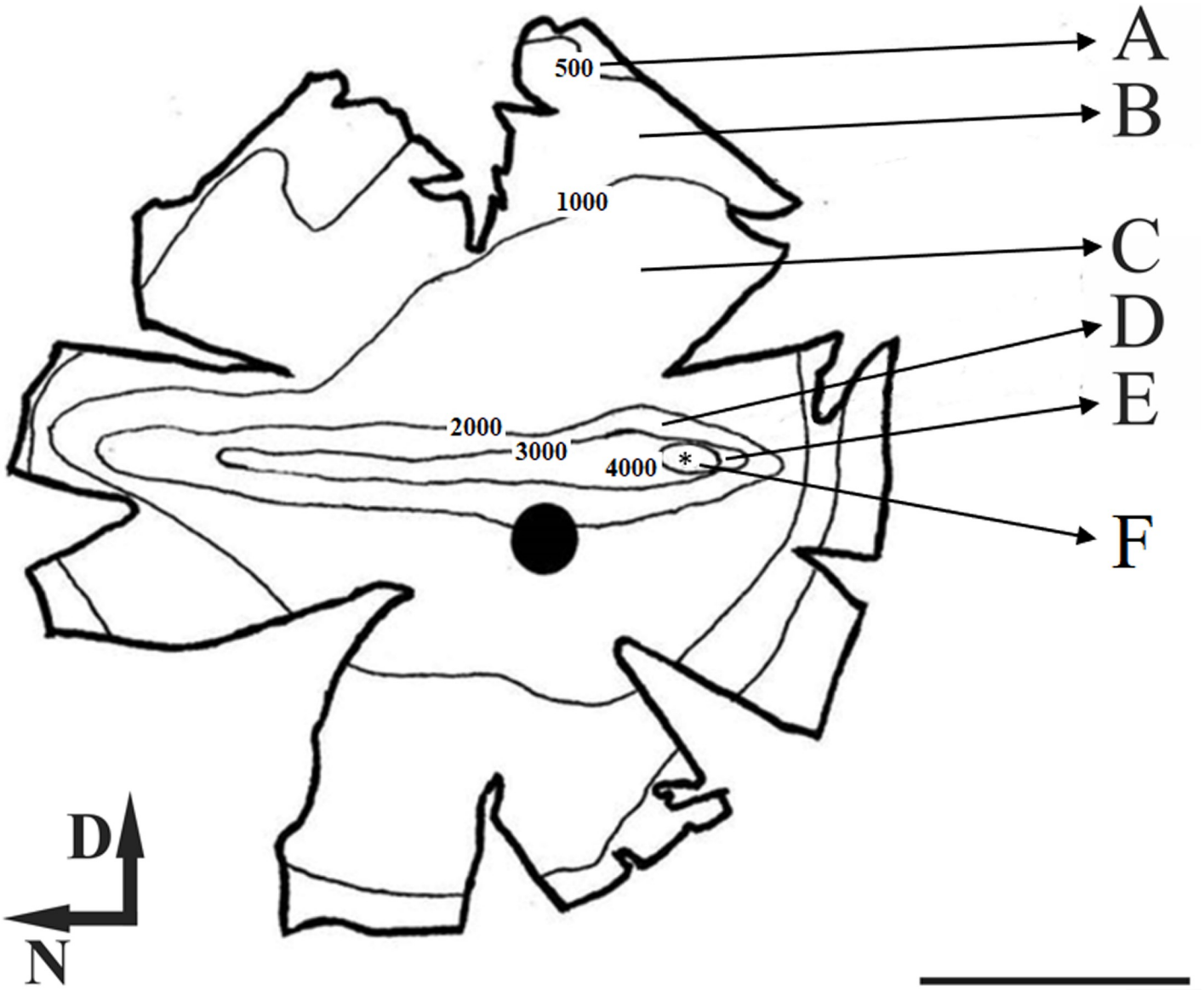

Fig 4. Ganglion cell mean isodensity map of peccary's retina. The contours correspond to the isodensity lines. The visual streak is visible by the horizontal elongation of the contours in the centro-dorsal retina. Each letter represents a different region of cellular density, (A) corresponded to the area between the wholemount border and the 500 GC/mm^2 contour. The (B) area between 500 and 1000 GC /mm^2; (C) area between 1000 and 2000 GC/mm^2; (D) region between 2000 and 3000 CG/mm^2; (E) region between 3000 and 4000 GC/mm^2, (F) region between 4000 GC/mm^2 and Peak density (*), (•) optic nerve. Scale bar = 5 mm.

https://doi.org/10.1371/journal.pone.0239719.g004

From the neurons in the ganglion cell layer the percentage of amacrine cells was always larger (reaching up to 70%) than the percentage of ganglion cells except for the *area temporalis* (Fig 9A). Notably, in the *area temporalis*, there was an inversion of the percentage of amacrine and ganglion cells where the amacrine cells decreased to 30.52% ± 3.91 on average against 69.48% ±3.09 of ganglion cells (Fig 9B).

Discussion

In the present study, we have investigated the density distribution of ganglion and displaced amacrine cells using six retinas from the collared peccary, a diurnal mammal found

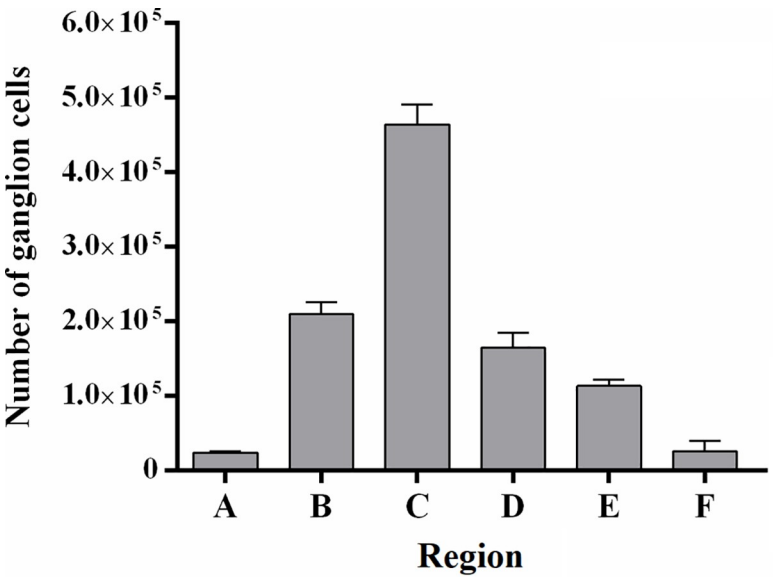

Fig 5. Number of ganglion cells by area. The A region corresponded to the area between the whole mount border and the 500 GC/mm^2 contour. The B region was the area between 500 and 1000 GC/mm^2; C region was the area between 1000 and 2000 GC/mm^2; D region was the area between 2000 and 3000 GC/mm^2; E region was the area between 3000 and 4000 GC/mm^2; F was the area between 4000 and 5000 GC/mm^2 and G region was the area on the peak density.

https://doi.org/10.1371/journal.pone.0239719.g005

throughout all Amazon Rainforest. The ganglion cell layer showed three characteristic regions with high cellular density: visual streak; *area temporalis* and a dorsotemporal extension named anakatabatic area, the later also found in other animals such as giraffe [32]. We located the visual streak above the optic nerve and the *area temporalis* superposed on the visual streak and the dorso temporal extension forming a dorsal arch of increased number of ganglion cells.

These results suggested that despite the difference in mean density values as well as peak density values, collared peccary and other species of the order Artiodactyla seem to share essential characteristics like retinal organization in ganglion cells layer. For example, in peccary, the mean cell density of ganglion cells in all retinas analyzed was 2253.5 GC/mm^2, this value is higher than was reported for the wild pig (*Sus scrofa*), whose mean density was about 1133 GC/mm^2 [31]. On the other hand, if we consider just the peak density value for collared peccary, the average was 6767±1.94 GC/mm^2, which is very close to what was found for wild pig's retina, that was 5735 ± 1066 GC/mm^2 [31]. Besides, the density peaks in both animals are displaced temporally relative to the optic nerve inside the visual streak. When our results for the collared peccary are compared to the retina topography analysis carried out in other species from the Artiodactyla order, some similarities are also noticed. For the goat, Gonzales-Soriano et al., reported a peak density of 3592 GC/mm^2 restricted to a circular area temporal to the optic disc, besides the existence of a visual streak [34]. In another study, this time in adult sheep retinas, the authors also found a visual streak formed by ganglion cells and *area temporalis* with a peak density of 18,000 GC/mm^2 [35]. These visual specializations (visual streak and *area temporalis*) were described in many artiodactyls such as giraffes [32], goats [41], cattle, pigs, and sheep [32, 33], animals that inhabit a variety of environments, from the savannah to dense rainforests. Whereas the dorsal extension was found in artiodactyls such as sheep [35], giraffes [32], and the Nubian ibex [42].

Coimbra et al., [32] argued based on the theory of phylogenetic ancestry of Stone [45] that, as the horizontal streak and area temporalis are frequent in retinas of artiodactyls, these

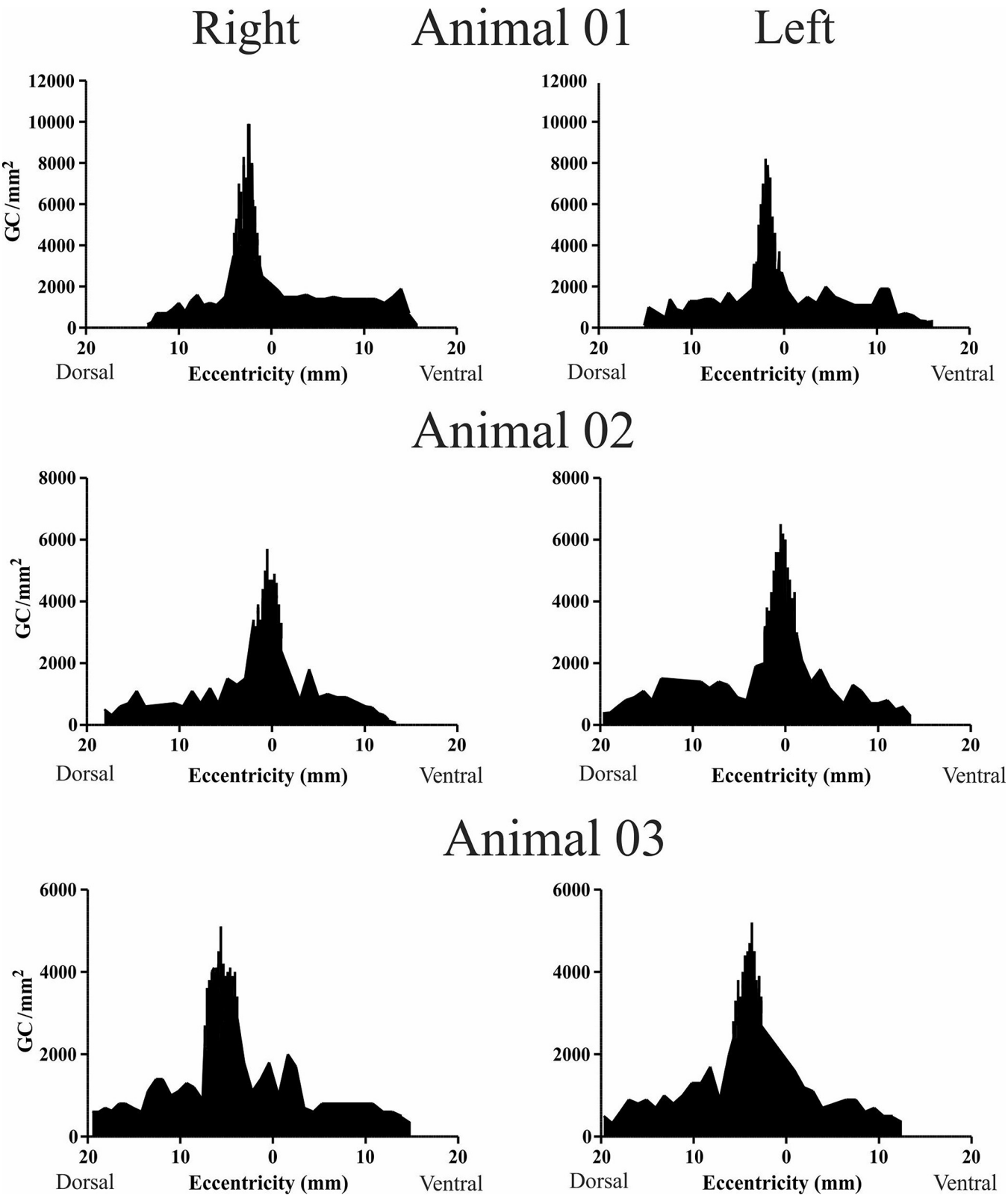

Fig 6. Ganglion cell density (cells/mm^2) along the vertical axis (dorso-ventral), perpendicular to the visual streak. Values in the x-axis indicate the distance in millimeters (mm) relative to the optic nerve (zero).

https://doi.org/10.1371/journal.pone.0239719.g006

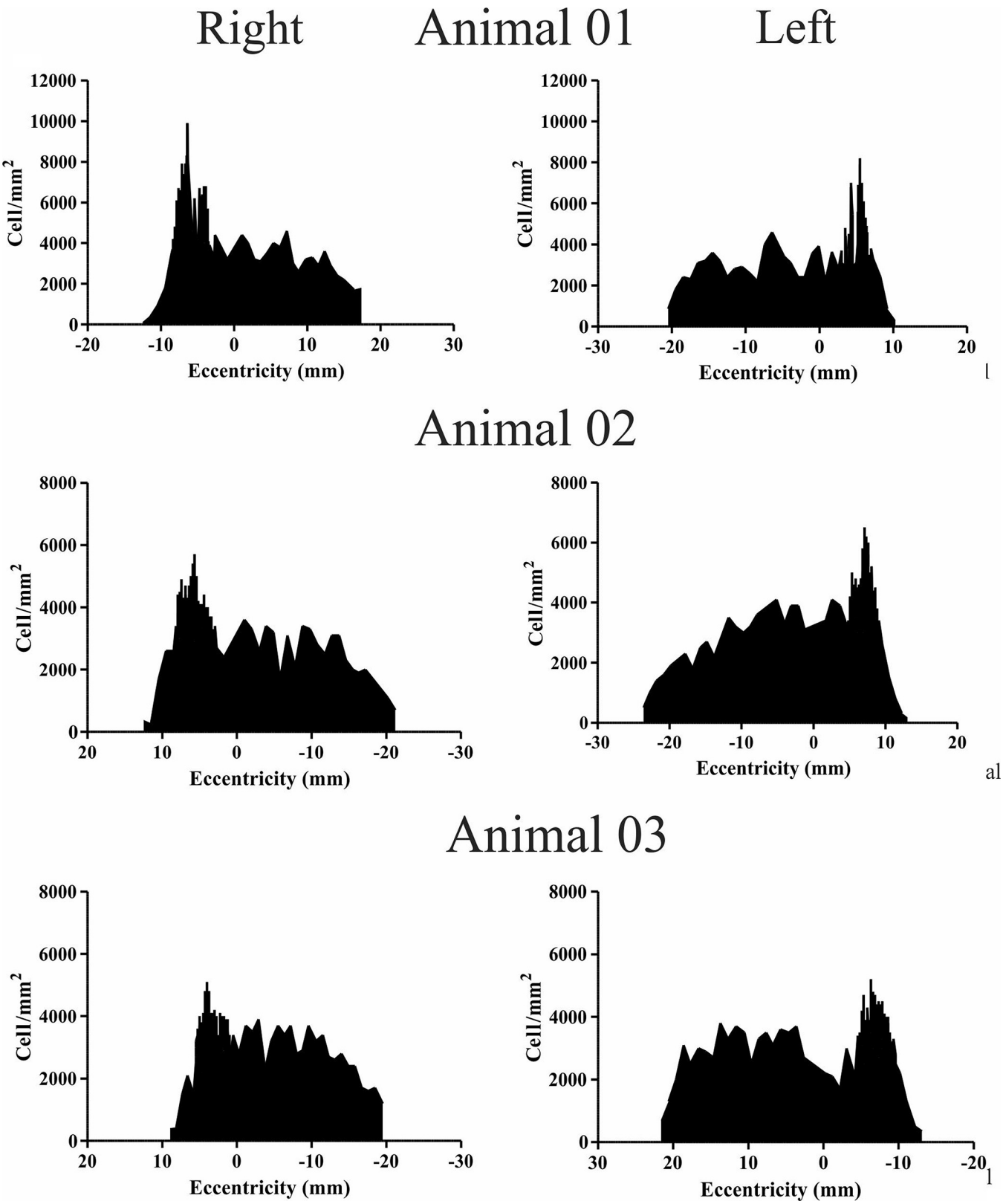

Fig 7. Ganglion cell density (cells/mm^2) along the horizontal axis (naso-temporal), along the visual streak. Values in the x axis indicate the distance in millimeters (mm) relative to the optic nerve (zero).

https://doi.org/10.1371/journal.pone.0239719.g007

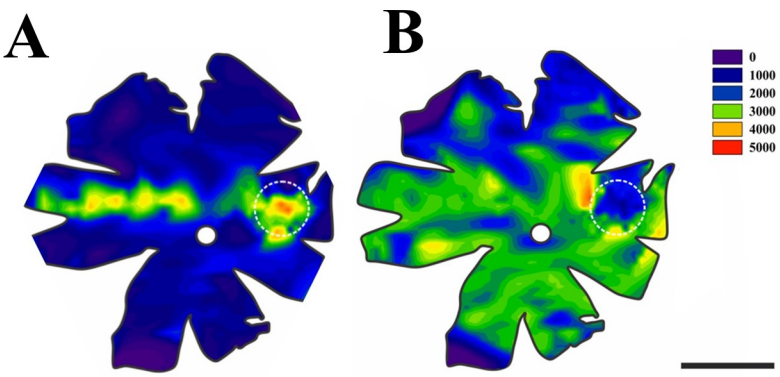

Fig 8. Mean cell density in the peccary's retina. The color scale on the right indicates density variation. **(A)** Ganglion cell density, the visual streak can be easily seen as a horizontal narrowly band in the naso-temporal axis. **(B)** Displaced amacrine cell density was approximately homogeneous overall retina surface. Interestingly, in the *area temporalis*, there was an intense decrease in the density of displaced amacrine cells. For both retinas, the *area temporalis* and the optic nerve is indicated by the white dotted circle and white disc, respectively. Scale bar = 5 mm.

https://doi.org/10.1371/journal.pone.0239719.g008

specializations are most likely plesiomorphic characters inherited from a common ancestor. Thus, regardless of habitat or lifestyle, the visual streak and area temporalis are conserved traits in the retina of the order [26, 31, 32, 34, 46]. Based on Hughes [47], Coimbra et al., [32] also claim that the joint presence of these two conspicuous retinal characteristics certainly indicates their relation with important behavioral marks like foraging and avoiding predators. The dorso-temporal extension forms a dorsal arch of ganglion cells increase Some authors reported that this specialization is closely related with demands required by the inferior visual field such as spotting predators, orientation during foraging or ambulation [32]. It was also found in other artiodactyl living in mountains and valleys [42], which points to a shared ecological niche.

Undoubtedly, independent of the topographical arrangement of retinal cells, the ubiquitous presence of the visual streak, dorsotemporal extension and area temporalis provide a good adaptation despite the variety of natural environments inhabited for these animals. In this respect, we can conclude that the distribution of ganglion cells in the retina of the collared peccary is not different from the distribution of ganglion cells observed in the retinas of other diurnal artiodactyls. Interestingly, the collared peccary is found in a wide range of

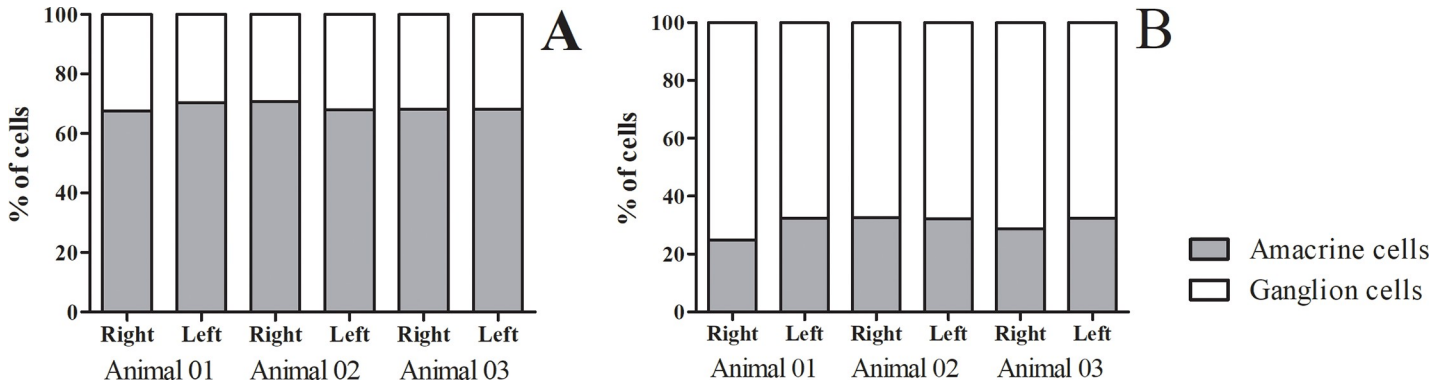

Fig 9. Stacked column graph of ganglion and amacrine cells for all six retinas studied. (A) Stacked column graph of percentage of amacrine and ganglion cells in the whole retina, except *area temporalis*. Each column represents 100% of cells in ganglion cell layer per retina, the percentage of amacrine cells is represented by the gray region and the percentage of ganglion cells is represented by white. It's noticeable that amacrine cells are in higher percentage than ganglion cells, the percentage of amacrine cells is around 70% and 30% for ganglion cells. **(B)** When just the *area temporalis* is considered, there was an inversion in the proportion of amacrine and ganglion cells. Ganglion cells were in a higher percentage than amacrine cells.

https://doi.org/10.1371/journal.pone.0239719.g009

Table 1. Retinal area, shrinkage and total ganglion cells number.

Retina	Eye	Area (mm^2)		Shrinkage	Total ganglion cells
		before	After		
Animal 01	Right	752	749	0.40%	994,818
Animal 01	Left	791	786	0.63%	907,666
Animal 02	Right	854	838	1.87%	889,134
Animal 02	Left	849	843	0.71%	1,154,780
Animal 03	Right	906	890	1.77%	1,055,662
Animal 03	Left	875	867	0.91%	1,174,927
Mean		837.8	828.8	1.05%	1,029,497
Std. Deviation		56.5	52.3	0.62%	121,060

https://doi.org/10.1371/journal.pone.0239719.t001

environments such as desertic regions and tropical forests, suggesting again that the topographical map described for ganglion cells serves well for different habitats being important for foraging and avoiding predators.

Displaced amacrine cells

The displaced amacrine cells have been reported in other species but with little emphasis on their topographical distribution [48–54]. The topography of amacrine cells in the collared peccary retina differs from ganglion cell distribution in some critical aspects related to the retina specializations, visual steak, dorsotemporal extension and *area temporalis*.

The topography of the amacrine cells displaced in the peccary's retina is almost homogeneous throughout its extension and does not form a retinal specialization. Except in the area centralis, the proportion of displaced amacrine cells in the ganglion cell layer of the peccary retina is higher than the proportion of ganglion cells. Likewise, displaced amacrine cells are absent from the central area in the retina of the teleost thraira [52]. In addition, studies of a variety of primate retinas have shown that the proportion of displaced amacrine cells in the peripheral retina is significantly higher than that in central retina [14, 55, 56].

In the howler monkey (*alouatta caraya*), a diurnal primate, the proportion of amacrine cells versus ganglion cells is like that found in the collared peccary. In the alouatta on the periphery of the retina, amacrine cells represent about 67% to 84% of the total cells in the ganglion cell layer. In contrast, in the central retina (fovea) there is an inversion in the proportion of amacrine and ganglion cells, and amacrine cells represent about 6% of the cells in that region [14]. In aotus, a nocturnal primate, the proportion of amacrine and ganglion cells is

Table 2. Descriptive statistics of the ganglion cell density for all six retinas.

		Animal 01		Animal 02		Animal 03	
		Right eye	Left eye	Right eye	Left eye	Right eye	Left eye
	Number of counting sites	331	318	372	318	433	437
Ganglion cells density (GC/mm^2)	Mean density	2634	2027	2276	2704	1890	1990
	Std. Deviation	2154	1876	1436	1536	1296	1371
	Std. Error of Mean	118.4	105.2	74.46	86.15	62.27	65.61
	Minimum	75	100	75	200	250	37
	25% Percentile	800	600	700	900	700	700
	Median	1700	1100	2700	3150	1500	1600
	75% Percentile	4200	3200	3400	3800	3100	3300
	Maximum (Peak of density)	9900	8200	5700	6500	5100	5200

https://doi.org/10.1371/journal.pone.0239719.t002

similar in most of the retina, except for the central region where displaced amacrine cells also decrease their percentage concerning ganglion cells [56].

The peculiarities and similarities found in the peccary' retina concerning other species, represent essential features of the order Artiodactyla to which the *P. tajacu* is inserted. The presence of retinal specializations in the peccary's retina, such as the visual streak, dorsotemporal extension and the *area temporalis*, which are directly related to its evolutionary history and ecology of the species, allow initiating morphophysiological comparisons of the retina of the collared peccary with that of other animal species.

Supporting information

S1 Dataset. Coordinates, density and percentage of ganglion and amacrine cells by Animal 01 Right.
(XLSX)

S2 Dataset. Coordinates, density and percentage of ganglion and amacrine cells by Animal 01 Left.
(XLSX)

S3 Dataset. Coordinates, density and percentage of ganglion and amacrine cells by Animal 02 Right.
(XLSX)

S4 Dataset. Coordinates, density and percentage of ganglion and amacrine cells by Animal 02 Left.
(XLSX)

S5 Dataset. Coordinates, density and percentage of ganglion and amacrine cells by Animal 03 Right.
(XLSX)

S6 Dataset. Coordinates, density and percentage of ganglion and amacrine cells by Animal 03 Left.
(XLSX)

Acknowledgments

One of the authors, Luiz Carlos de Lima Silveira, sadly passed away before the submission of the final version of this manuscript. Fernando Allan de Farias Rocha accepts responsibility for the integrity and validity of the data collected and analyzed. Luiz was one of the researchers to lead the rise of the first neuroscience group in Brazilian Amazon. He was, directly and indirectly, responsible for the formation of more than a dozen active researchers in the field of visual neuroscience, including the authors of the current article. His passion for science and its transforming life nature, especially in a poor region, will be always remembered. Thank you Professor Luiz Carlos.

Author Contributions

Conceptualization: Fernando Allan de Farias Rocha.

Data curation: Givago da Silva Souza.

Formal analysis: Kelly Helorany Alves Costa, Bruno Duarte Gomes, Luiz Carlos de Lima Silveira, Isabelle Christine Vieira da Silva Martins, Eliza Maria da Costa Brito Lacerda, Fernando Allan de Farias Rocha.

Funding acquisition: Fernando Allan de Farias Rocha.

Investigation: Kelly Helorany Alves Costa.

Methodology: Kelly Helorany Alves Costa, Bruno Duarte Gomes, Luiz Carlos de Lima Silveira, Isabelle Christine Vieira da Silva Martins, Eliza Maria da Costa Brito Lacerda, Fernando Allan de Farias Rocha.

Project administration: Fernando Allan de Farias Rocha.

Software: Fernando Allan de Farias Rocha.

Supervision: Luiz Carlos de Lima Silveira, Givago da Silva Souza, Fernando Allan de Farias Rocha.

Writing – original draft: Kelly Helorany Alves Costa, Fernando Allan de Farias Rocha.

Writing – review & editing: Bruno Duarte Gomes, Givago da Silva Souza, Fernando Allan de Farias Rocha.

References

1. Do-Nascimento JL, Do-Nascimento RS, Damasceno BA, Silveira LC. The neurons of the retinal ganglion cell layer of the guinea pig: quantitative analysis of their distribution and size. Braz J Med Biol Res. 1991; 24: 199–214. PMID: 1726652
2. Lima SM, Silveira LC, Perry VH. Distribution of M retinal ganglion cells in diurnal and nocturnal New World monkeys. J Comp Neurol. 1996; 368: 538–52. https://doi.org/10.1002/(SICI)1096-9861(19960513)368:4<538::AID-CNE6>3.0.CO;2-5 PMID: 8744442
3. da Rocha EG, Freire MAM, Bahia CP, Pereira A, Sosthenes MCK, Silveira LCL, et al. Dendritic structure varies as a function of eccentricity in V1: a quantitative study of NADPH diaphorase neurons in the diurnal South American rodent agouti, Dasyprocta prymnolopha. Neuroscience. 2012; 216: 94–102. https://doi.org/10.1016/j.neuroscience.2012.04.042 PMID: 22542676
4. Dias IA, Bahia CP, Franca JG, Houzel JC, Lent R, Mayer AO, et al. Topography and architecture of visual and somatosensory areas of the agouti. J Comp Neurol. 2014; 522: 2576–2593. https://doi.org/10.1002/cne.23550 PMID: 24477926
5. dos Reis JWL, de Carvalho WA, Saito CA, Silveira LCL. Morphology of horizontal cells in the retina of the capuchin monkey, Cebus apella: how many horizontal cell classes are found in dichromatic primates? J Comp Neurol. 2002; 443: 105–123. PMID: 11793350
6. Dos Santos SN, Dos Reis JWL, Da Silva Filho M, Kremers J, Silveira LCL. Horizontal cell morphology in nocturnal and diurnal primates: a comparison between owl-monkey (Aotus) and capuchin monkey (Cebus). Vis Neurosci. 2005; 22: 405–415. https://doi.org/10.1017/S0952523805224033 PMID: 16212699
7. Elston GN, Elston A, Aurelio-Freire M, Gomes Leal W, Dias IA, Pereira AJ, et al. Specialization of pyramidal cell structure in the visual areas V1, V2 and V3 of the South American rodent, Dasyprocta primnolopha. Brain Res. 2006; 1106: 99–110. https://doi.org/10.1016/j.brainres.2006.05.100 PMID: 16854386
8. Finlay BL, Franco ECS, Yamada ES, Crowley JC, Parsons M, Muniz JAPC, et al. Number and topography of cones, rods and optic nerve axons in New and Old World primates. Vis Neurosci. 2008; 25: 289–299. https://doi.org/10.1017/S0952523808080371 PMID: 18598400
9. Freire MAM, Rocha EG, Oliveira JLF, Guimaraes JS, Silveira LCL, Elston GN, et al. Morphological variability of NADPH diaphorase neurons across areas V1, V2, and V3 of the common agouti. Brain Res. 2010; 1318: 52–63. https://doi.org/10.1016/j.brainres.2009.12.045 PMID: 20036219
10. Goulart PRK, Bonci DMO, Galvao O de F, Silveira LC de L, Ventura DF. Color discrimination in the tufted capuchin monkey, Sapajus spp. PLoS One. 2013; 8: e62255. https://doi.org/10.1371/journal.pone.0062255 PMID: 23620819

11. Kilavik BE, Silveira LCL, Kremers J. Spatial receptive field properties of lateral geniculate cells in the owl monkey (Aotus azarae) at different contrasts: a comparative study. Eur J Neurosci. 2007; 26: 992–1006. https://doi.org/10.1111/j.1460-9568.2007.05709.x PMID: 17714192

12. Lameirao SVOC Hamassaki DE, Rodrigues AR DE Lima SMA, Finlay BL Silveira LCL. Rod bipolar cells in the retina of the capuchin monkey (Cebus apella): characterization and distribution. Vis Neurosci. 2009; 26: 389–396. https://doi.org/10.1017/S0952523809990186 PMID: 19709465

13. Picanco-Diniz CW, Oliveira HL, Silveira LC, Oswaldo-Cruz E. The visual cortex of the agouti (Dasyprocta aguti): architectonic subdivisions. Braz J Med Biol Res. 1989; 22: 121–138. PMID: 2758167

14. Muniz JAPC, de Athaide LM, Gomes BD, Finlay BL, Silveira LC de L. Ganglion cell and displaced amacrine cell density distribution in the retina of the howler monkey (Alouatta caraya). PLoS One. 2014; 9: e115291. https://doi.org/10.1371/journal.pone.0115291 PMID: 25546077

15. Silveira LCL, Saito CA, da Silva Filho M, Kremers J, Bowmaker JK, Lee BB. Alouatta trichromatic color vision: cone spectra and physiological responses studied with microspectrophotometry and single unit retinal electrophysiology. PLoS One. 2014; 9: e113321. https://doi.org/10.1371/journal.pone.0113321 PMID: 25405863

16. Picanco-Diniz CW, Silveira LC, de Carvalho MS, Oswaldo-Cruz E. Contralateral visual field representation in area 17 of the cerebral cortex of the agouti: a comparison between the cortical magnification factor and retinal ganglion cell distribution. Neuroscience. 1991; 44: 325–333. https://doi.org/10.1016/0306-4522(91)90057-u PMID: 1944888

17. Silveira LC, Picanço-Diniz CW, Oswaldo-Cruz E. Distribution and size of ganglion cells in the retinae of large Amazon rodents. Vis Neurosci. 1989; 2: 221–235. https://doi.org/10.1017/s0952523800001140 PMID: 2562148

18. Silveira LC, Yamada ES, Picanco-Diniz CW. Displaced horizontal cells and biplexiform horizontal cells in the mammalian retina. Vis Neurosci. 1989; 3: 483–488. https://doi.org/10.1017/s0952523800005988 PMID: 2487119

19. Yamada ES, Silveira LC. Neurofibrillar bipolar cells in the capybara retina. Vis Neurosci. 1996; 13: 1173–1177. https://doi.org/10.1017/s0952523800007811 PMID: 8961546

20. de Lima SMA, Ahnelt PK, Carvalho TO, Silveira JS, Rocha FAF, Saito CA, et al. Horizontal cells in the retina of a diurnal rodent, the agouti (Dasyprocta aguti). Vis Neurosci. 2005; 22: 707–720. https://doi.org/10.1017/S0952523805226032 PMID: 16469182

21. Rocha FA de F, Ahnelt PK, Peichl L, Saito CA, Silveira LCL, De Lima SMA. The topography of cone photoreceptors in the retina of a diurnal rodent, the agouti (Dasyprocta aguti). Vis Neurosci. 2009; 26: 167–175. https://doi.org/10.1017/S095252380808098X PMID: 19250601

22. da Fontoura Costa L, Rocha F, Araujo de Lima SM. Characterizing polygonality in biological structures. Phys Rev E Stat Nonlin Soft Matter Phys. 2006; 73: 11913.

23. Braekevelt CR. Fine structure of the retinal rods and cones in the domestic pig. Graefes Arch Clin Exp Ophthalmol. 1983; 220: 273–278. https://doi.org/10.1007/BF00231355 PMID: 6629020

24. Neitz J, Jacobs GH. Spectral sensitivity of cones in an ungulate. Vis Neurosci. 1989; 2: 97–100. https://doi.org/10.1017/s0952523800011949 PMID: 2487648

25. Jacobs GH, Deegan JF, Neitz J, Murphy BP, Miller K V., Marchinton RL. Electrophysiological measurements of spectral mechanisms in the retinas of two cervids: white-tailed deer (Odocoileus virginianus) and fallow deer (Dama dama). J Comp Physiol A. 1994; 174: 551–557. https://doi.org/10.1007/BF00217375 PMID: 8006855

26. JACOBS GH, DEEGAN JF, NEITZ J. Photopigment basis for dichromatic color vision in cows, goats, and sheep. Visual Neuroscience. ENGLAND; 1998. pp. 581–584. https://doi.org/10.1017/s0952523898153154 PMID: 9685209

27. Chandler MJ, Smith PJ, Samuelson D a, MacKay EO. Photoreceptor density of the domestic pig retina. Vet Ophthalmol. 1999; 2: 179–184. vop077 [pii] https://doi.org/10.1046/j.1463-5224.1999.00077.x PMID: 11397262

28. Ahnelt PK, Ahnelt PK, Kolb H, Kolb H. The mammalian photoreceptor mosaic adaptive design. Prog Retin Eye Res. 2000; 19: 711. https://doi.org/10.1016/s1350-9462(00)00012-4 PMID: 11029553

29. Hendrickson A, Hicks D. Distribution and density of medium- and short-wavelength selective cones in the domestic pig retina. Exp Eye Res. 2002; 74: 435–444. https://doi.org/10.1006/exer.2002.1181 PMID: 12076087

30. Hebel R. Distribution of retinal ganglion cells in five mammalian species (pig, sheep, ox, horse, dog). Anat Embryol (Berl). 1976; 150: 45–51. https://doi.org/10.1007/BF00346285 PMID: 1015629

31. García M, Ruiz-Ederra J, Hernández-Barbáchano H, Vecino E. Topography of pig retinal ganglion cells. J Comp Neurol. 2005; 486: 361–372. https://doi.org/10.1002/cne.20516 PMID: 15846788

32. Coimbra JP, Hart NS, Collin SP, Manger PR. Scene from above: Retinal ganglion cell topography and spatial resolving power in the giraffe (Giraffa camelopardalis). J Comp Neurol. 2013; 521: 2042–2057. https://doi.org/10.1002/cne.23271 PMID: 23595815

33. Luck CP. The comparative morphology of the eyes of certain African Suiformes. Vision Res. 1966; 5: 283–297. https://doi.org/10.1016/0042-6989(65)90005-2 PMID: 5905870

34. Gonzalez-Soriano J, Mayayo-Vicente S, Martinez-Sainz P, Contreras-Rodriguez J, Rodriguez-Veiga E. A quantitative study of ganglion cells in the goat retina. Anat Histol Embryol. 1997; 26: 39–44. https://doi.org/10.1111/j.1439-0264.1997.tb00101.x PMID: 9178578

35. Shinozaki A, Hosaka Y, Imagawa T, Uehara M. Topography of ganglion cells and photoreceptors in the sheep retina. J Comp Neurol. 2010; 518: 2305–2315. https://doi.org/10.1002/cne.22333 PMID: 20437529

36. Garza-Gisholt E, Hemmi JM, Hart NS, Collin SP. A comparison of spatial analysis methods for the construction of topographic maps of retinal cell density. PLoS One. 2014. https://doi.org/10.1371/journal.pone.0093485 PMID: 24747568

37. Ebersole JP. Javelinas and Other Peccaries: Their Biology, Management, and Use. Lyle K. Sowls. Q Rev Biol. 1998; 73: 84–85. https://doi.org/10.1086/420109

38. Bissonette JA. Sowls L. K. The Peccaries. Univ. Arizona Press, Tucson, xvi + 251 pp., illustrated, 1984. Journal of Mammalogy. 1986. pp. 616–617.

39. Ezra-Elia R, Ross M, Avni-Magen N, Berkowitz A, Ofri R. The retina of the collared peccary (Pecari tajacu): structure and function. Vet Ophthalmol. 2018; 0. https://doi.org/10.1111/vop.12548 PMID: 29336116

40. Stone J. The number and distribution of ganglion cells in the cat's retina. J Comp Neurol. 1978; 180: 753–771. https://doi.org/10.1002/cne.901800407 PMID: 681546

41. Hughes A. Population magnitudes and distribution of the major modal classes of cat retinal ganglion cell as estimated from HRP filling and a systematic survey of the soma diameter spectra for classical neurones. J Comp Neurol. 1981; 197: 303–339. https://doi.org/10.1002/cne.901970209 PMID: 7276237

42. Coimbra JP, Alagaili AN, Bennett NC, Mohammed OB, Manger PR. Unusual topographic specializations of retinal ganglion cell density and spatial resolution in a cliff-dwelling artiodactyl, the Nubian ibex (Capra nubiana). J Comp Neurol. 2019. https://doi.org/10.1002/cne.24709 PMID: 31045240

43. Coimbra JP, Bertelsen MF, Manger PR. Retinal ganglion cell topography and spatial resolving power in the river hippopotamus (Hippopotamus amphibius). J Comp Neurol. 2017. https://doi.org/10.1002/cne.24179 PMID: 28139828

44. Hughes A, Whitteridge D. The receptive fields and topographical organization of goat retinal ganglion cells. Vision Res. 1973; 13: 1101–1114. https://doi.org/10.1016/0042-6989(73)90147-8 PMID: 4713921

45. Stone J. Parallel processing in the visual system: the classification of retinal ganglion cells and its impact on the neurobiology of vision. New York: Plenum Press; 1983.

46. Braekevelt CR. Retinal photoreceptor fine structure in the domestic sheep. Acta Anat (Basel). 1983; 116: 265–275. https://doi.org/10.1159/000145750 PMID: 6880602

47. Hughes A. The Topography of Vision in Mammals of Contrasting Life Style: Comparative Optics and Retinal Organisation. In: Crescitelli F, editor. The Visual System in Vertebrates. Berlin, Heidelberg: Springer Berlin Heidelberg; 1977. pp. 613–756. https://doi.org/10.1007/978-3-642-66468-7_11

48. Ball AK, Dickson DH. Displaced amacrine and ganglion cells in the newt retina. Exp Eye Res. 1983; 36: 199–213. https://doi.org/10.1016/0014-4835(83)90006-4 PMID: 6825738

49. Keyser KT, Macneil MA, Dmitrieva N, Wang F, Masland RH, Lindstrom JM. Amacrine, ganglion, and displaced amacrine cells in the rabbit retina express nicotinic acetylcholine receptors. Vis Neurosci. 2000. https://doi.org/10.1017/S095252380017508X PMID: 11153654

50. Perry VH, Walker M. Amacrine cells, displaced amacrine cells and interplexiform cells in the retina of the rat. Proc R Soc Lond B Biol Sci. 1980. https://doi.org/10.1098/rspb.1980.0060 PMID: 6158054

51. Wässle H, Chun MH, Müller F. Amacrine cells in the ganglion cell layer of the cat retina. J Comp Neurol. 1987. https://doi.org/10.1002/cne.902650308 PMID: 3693612

52. Costa LDF, Bonci DMO, Saito CA, Rocha FADF, Silveira LCDL, Ventura DF. Voronoi analysis uncovers relationship between mosaics of normally placed and displaced amacrine cells in the thraira retina. Neuroinformatics. 2007. https://doi.org/10.1385/NI: 5:1:59

53. Müller LPDS, Shelley J, Weiler R. Displaced amacrine cells of the mouse retina. J Comp Neurol. 2007. https://doi.org/10.1002/cne.21487 PMID: 17853452

54. Curcio CA, Allen KA. Topography of ganglion cells in human retina. J Comp Neurol. 1990. https://doi.org/10.1002/cne.903000103 PMID: 2229487

55. Wässle H, Grünert U, Röhrenbeck J, Boycott BB. Retinal ganglion cell density and cortical magnification factor in the primate. Vision Res. 1990. https://doi.org/10.1016/0042-6989(90)90166-I

56. Silveira LCL, Perry VH, Yamada ES. The retinal ganglion cell distribution and the representation of the visual field in area 17 of the owl monkey, Aotus trivirgatus. Vis Neurosci. 1993. https://doi.org/10.1017/S095252380000609X PMID: 8217938